Appl Biochem Biotechnol (2013) 171:1513–1524
DOI 10.1007/s12010-013-0442-5

Response of Human Mesenchymal Stem Cells to Patterned and Randomly Oriented Poly(Vinyl Alcohol) Nano-fibrous Scaffolds Surface-Modified with Arg-Gly-Asp (RGD) Ligand

Yasaman Zamani · Mohammad Rabiee · Mohammad Ali Shokrgozar · Shahin Bonakdar · Mohammadreza Tahriri

Received: 6 June 2013 / Accepted: 6 August 2013 /
Published online: 21 August 2013

Abstract The aim of this study was to obtain a better insight of how nano-fibrous scaffolds can affect human mesenchymal stem cells responses. Therefore, in this study, using electrospinning technique, poly(vinyl alcohol) (PVA) nano-fibers with two different patterns were prepared. In the first structure, PVA nano-fibers were oriented randomly and in the second structure, nano-fibers were electrospun in such a way that a special pattern was obtained. In order to enhance their stability, scaffolds were cross-linked using glutaraldehyde vapor. RGD immobilization was used to improve cell adhesion properties of the scaffolds. SEM micrographs demonstrated that the cell adhesion was effectively enhanced after RGD immobilization and higher cell densities were observed on RGD-modified scaffolds. Randomly oriented nano-fibers showed better cell adhesion compared to patterned structure. Patterned structure also revealed slightly lower cell viability compared to random nano-fibers. Finally, it was assumed that randomly oriented nano-fibers provide a more favorable surface for cells.

Keywords PVA · Electrospun nano-fibers · Surface · Pattern · RGD ligand · hMSCs response

Introduction

In recent years, topographical strategies have been receiving increasing attention in the development of tissue engineering scaffolds [1, 2]. It is accepted that the role of scaffolds is

Y. Zamani · M. Rabiee · M. Tahriri
Biomaterial Group, Faculty of Biomedical Engineering, Amirkabir University of Technology, Hafez Ave, Tehran 15875-4413, Iran

M. A. Shokrgozar · S. Bonakdar
National Cell Bank of Iran, Pasteur Institute of Iran, 69 Pasteur Ave, Tehran 1316943551, Iran

M. Tahriri (✉)
Dental Materials Department, School of Dentistry, Tehran University of Medical Sciences (TUMS), Tehran, Iran
e-mail: m-tahriri@aut.ac.ir

more than only providing mechanical support; but they act as intelligent surfaces capable of providing chemical and topographical signals to guide cells [3]. Surface topography plays a key role in modulating cell behaviors, such as cell adhesion and spreading, which can in turn influence cell viability, morphology, and differentiation [4–6]. Therefore, recently a wide range of studies have focused on the interaction of cells with model substrates in an effort to understand the effect of scaffold surface topography on the behavior of adherent cells [1, 3, 7, 8].

It has been demonstrated previously that cell adhesion is cooperatively regulated by the surface topography and the presence of cell recognition ligands on the surface [4]. In order to improve biological properties of synthetic polymers, cell adhesive proteins and polysaccharides such as collagen, chitosan, silk fibroin, and RGD have been coated on the surface of nano-fibrous matrices [9, 10]. However, immobilization of small RGD moieties on the surface seems to be more advantageous than the protein-coating method for improving cell adhesion behaviors, because the surface immobilization of cell-adhesive ligands provides higher stability, non-immune response, and the ability of selective adhesion of a particular cell type [11]. Surface-engineered nano-fibrous matrices have exhibited enhancement in cell adhesion, spreading, and proliferation. They also showed high cell densities because of their higher surface area-to-volume ratio than that in the unmodified substrates [9, 10]. From this perspective, we immobilized RGD peptides to the surface of nano-fibrous scaffolds for enhancing their cytocompatibility.

Cells in their native environment interact with extracellular matrix (ECM) components in the nanometer size (50–500 nm diameter fibers) [2, 12]. It has long been hypothesized that in order to design an ideal scaffold which can duplicate all of the essential intercellular reactions and promote native intracellular responses, the natural ECM must be mimicked. Thus, considerable attention has been directed toward nano-fibrous matrices due to their ability to interact with cells in a manner that mimics the natural ECM. These nano-fibrous scaffolds have several advantages such as large surface area, pore sizes ranging from several to tens of micrometers, adjustable porosities up to more than 90 %, and controlled mechanical properties [12–15].

Electrospinning, a facile, efficient, and inexpensive polymer-processing method, has been proved as an effective way in creating nanometer-scale fibers. A wide variety of natural materials such as chitosan [16], silk [17], collagen [18], gelatin [6], and a wide range of synthetic polymers like poly(vinyl alcohol) (PVA), polycaprolactone (PCL), poly(L-lactic acid), and co-polymers such as poly(lactic-co-glucolic acid) have been electrospun as tissue-engineering scaffolds [19–22]. The resultant structure resembles the collagen fiber network existing in the natural ECM. The electrospun fibers can be patterned by collecting the fibers on different targets, creating surfaces endowed with topographical cues at the nanometer scale. Surface patterning is an approach that has been studied over a number of years as a method for improving some scaffold characteristics such as the ability of water retention and guiding the behavior of cell attachment. There is abundant evidence that features like grooves [23], pits [8], and pillars [3] have several effects on the function of different cells. Wilkinson et al. suggested the use of materials with nano and micro metric patterns in cellular engineering. They concluded that cells are profoundly affected by surface topography and by patterned surface chemistry [23]. In one study, Anderson et al. fabricated two different nano-structures and compared them with flat film control. Results showed that nano-scale topography can affect the morphology and function of adherent cells [24]. Dalby et al. investigated the response of osteoprogenitors to semi-ordered and random nano-topographies. They found that nano-topography is an important factor in mesenchymal differentiation and in the design of scaffolds [25]. In the next study, they demonstrated that highly ordered nano-topographies produce low to negligible cellular adhesion and

osteoblastic differentiation. On the other hand, cells on random nano-topographies exhibited a more osteoblastic morphology [7]. In another study by Mikos et al., the spreading of rat mesenchymal stem cells (MSCs) was promoted by nano-fibers, while cell attachment did not seem to be enhanced [26]. In a recent study by He et al. regarding the effect of nano-fiber diameter and pattern on stem cells, the best fiber diameter for cell viability and proliferation was different for aligned and random nano-fibers. In the sample with aligned fibers, cell viability and proliferation was best on 500 nm fibers, and reduced on smaller or larger fibers. However, on random fibers cell viability and proliferation was best with the smallest (350 nm) and largest (1,150 nm) diameter fibers [1].

As described above, numerous studies regarding the effect of scaffold surface topography on adherent cells have been performed. In this case, features like grooves, ridges, pillars, etc. are often created on the surface and properties such as cell adhesion, orientation, morphology, proliferation, and differentiation are investigated on these engineered surfaces [2, 3, 24, 27, 28]. In this study, nano-fibrous scaffolds are fabricated by electrospinning using different collectors. PVA was used to fabricate three different substrate types: flat film (as a control), patterned, and randomly oriented nano-fibers. PVA is a synthetic water-soluble polymer that has been studied intensively because of its biocompatibility, non-toxicity, processability, and good chemical and thermal stability [29, 30]. Furthermore, electrospinning of PVA has been studied extensively due to its good fiber-forming properties and the use of water-based solvents in this process [10, 18]. The prepared substrates were cross-linked using glutaraldehyde (GTA) vapor to enhance their water stability and RGD immobilized to improve their cell attachment properties. Finally, human mesenchymal stem cells (hMSCs) were seeded onto the scaffolds to study their response in terms of cell attachment, morphology, and viability.

Materials and Methods

Electrospinning Process

Poly(vinyl alcohol) (degree of hydrolysis 99 %, Mw=72,000) was obtained from Merck, Germany. PVA solution of 12 wt% was prepared by dissolving 1.2 g of PVA powder in 10 ml distilled water with moderate stirring at 90 °C for 3 h. The PVA solution (2 ml) was put into a 10-ml syringe with a stainless steel needle (19G, inner diameter, 0.3 mm) attached at the open end. The polymer solution was fed into the syringe using a syringe pump (New Eva Pump System Inc., USA) at a flow rate of 0.5 ml/h with an applied voltage of 15 kV (Gamma High Research, USA). Randomly oriented nano-fibers were collected on a flat collector plate wrapped with aluminum foil. Patterned nano-fibers were formed by replacing the aluminum foil with a stainless steel mesh with pore diameter of 90 μm. The fiber collector was kept at a distance of 15 cm from the needle tip.

Film Preparation

Thin films of PVA were prepared by casting the solution into a polystyrene Petri dish. These films were dried under atmospheric temperature for 3 days, following a vacuum at 50 °C for another day.

Morphology of Electrospun Scaffolds

The patterned and randomly oriented structures of the nano-fibrous scaffolds were confirmed by scanning electron microscopy (SEM, Philips XL-30). The samples were sputter

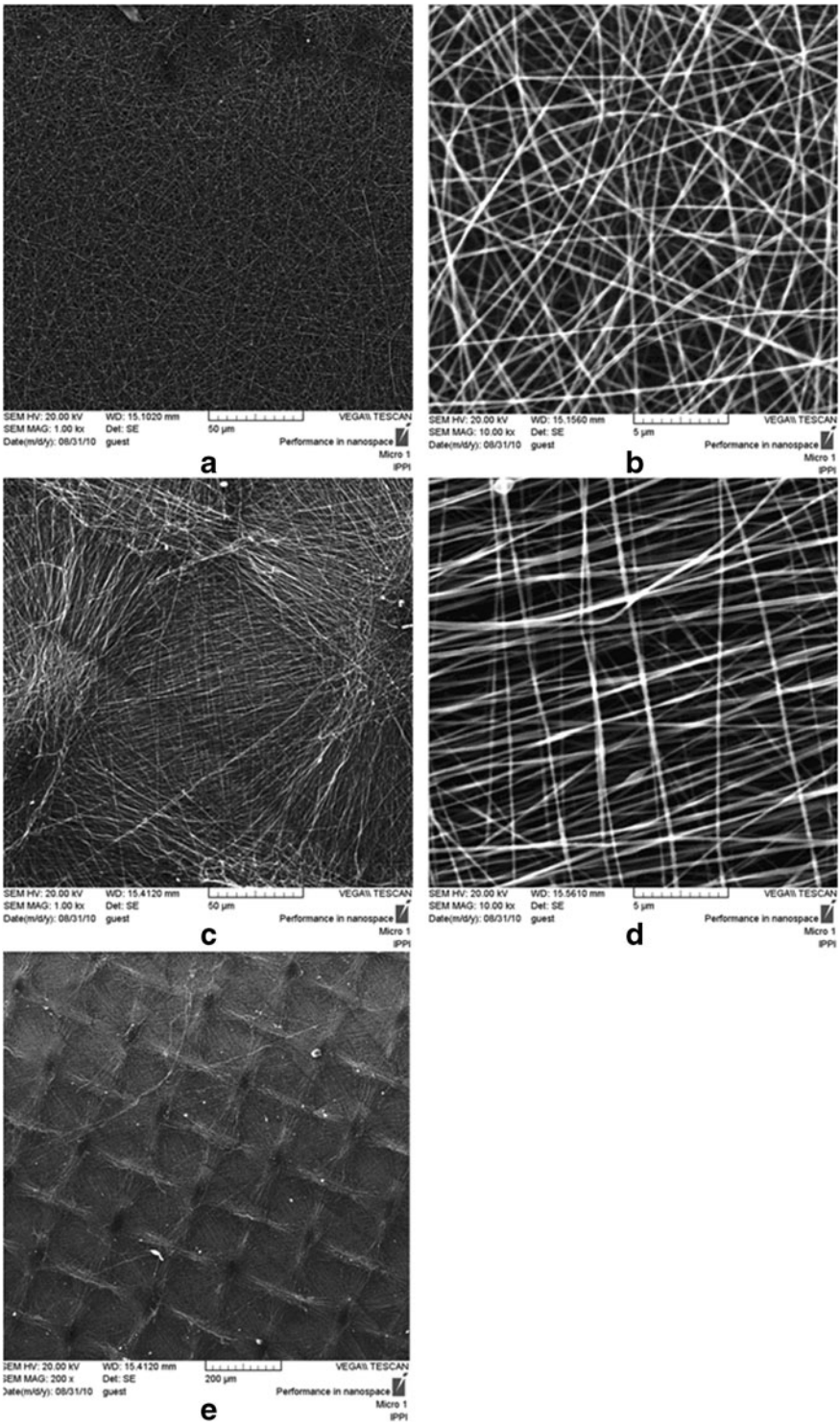
SEM HV: 20.00 kV
SEM MAG: 1.00 kx
Date(m/d/y): 08/31/10
WD: 15.1020 mm
Det: SE
guest
50 µm
VEGA\\ TESCAN
Performance in nanospace
Micro 1
IPPI
a
SEM HV: 20.00 kV
SEM MAG: 10.00 kx
Date(m/d/y): 08/31/10
WD: 15.1560 mm
Det: SE
guest
5 µm
VEGA\\ TESCAN
Performance in nanospace
Micro 1
IPPI
b
SEM HV: 20.00 kV
SEM MAG: 1.00 kx
Date(m/d/y): 08/31/10
WD: 15.4120 mm
Det: SE
guest
50 µm
VEGA\\ TESCAN
Performance in nanospace
Micro 1
IPPI
c
SEM HV: 20.00 kV
SEM MAG: 10.00 kx
Date(m/d/y): 08/31/10
WD: 15.5610 mm
Det: SE
guest
5 µm
VEGA\\ TESCAN
Performance in nanospace
Micro 1
IPPI
d
EM HV: 20.00 kV
EM MAG: 200 x
)ate(m/d/y): 08/31/10
WD: 15.4120 mm
Det: SE
guest
200 µm
VEGA\\ TESCAN
Performance in nanospace
Micro 1
IPPI
e

◀ **Fig. 1** Scanning electron micrographs of randomly oriented (**a** and **b**) and patterned (**c**, **d**, and **e**) PVA electrospun nano-fibers at different magnifications: **a** and **c** ×1,000, **b** and **d** ×2,000, **e** ×200

coated with gold before scanning. The average fiber diameter of the electrospun nano-fibers were measured by Adobe Photoshop 7.0 software from the SEM micrographs.

Cross-linking

The samples were subjected to cross-linking process in order to enhance their stability for cell culture studies. All the specimens were cut into 1 cm^2 pieces and allowed to keep under GTA vapor (25 % aqueous solution, Merck, Germany) for 120 h in a desiccator. The samples were then vacuumed at 40 °C for 24 h followed by further heating at 50 °C for another 24 h.

RGD Immobilization

Cell adhesion ligand Arg-Gly-Asp (RGD, Sigma, Germany) was immobilized onto the surface of the cross-linked specimens to enhance their cell attachment properties. The details of this procedure have been described elsewhere [31]. Briefly, isocyanate groups were first introduced onto the scaffold surface by placing the dried specimens in a flask with a toluene solution containing 1 wt% hexamethylene diisocyanate (Merck, Germany). After purging with nitrogen gas, the reaction mixture was gently stirred at 25 °C for 90 min. The scaffolds with the introduced isocyanate groups were then immersed in RGD solution at room temperature for 180 min to affect the covalent immobilization.

PBS Absorption

The known weight of specimens were placed in closed bottles containing 5 ml of phosphate buffered saline (PBS, pH=7.4) and incubated in vitro at 37 °C for 24 h. The wet weight of the specimens was determined by weighing them immediately after removing the specimens from PBS and blotting with filter paper to absorb water on the scaffold surface. The water uptake of the scaffolds in PBS was then calculated from the formula:

$$A(\%) = [(W_1 - W_0)/W_0] \times 100$$

Where A is PBS absorption and W_1 and W_0 are the weights of scaffolds before and after immersion in the medium, respectively.

Cell Culture of hMSCs

Adipose tissue taken from informed 23-year-old patient's abdominal area was washed with PBS containing antibiotics (1 % penicillin–streptomycin; Gibco). Tissue was transferred to a tissue culture Petri dish and chopped to tiny pieces. Chopped tissues were then discharged to a PBS containing tube and centrifuged at 1,400 rpm for 5 min. The red blood cells were settled at the bottom and the adipose tissue floated at the top of the tube. The adipose tissue was transferred to another tube containing 2 mg/ml collagenase (sigma) and incubated at 37 °C for 30 min. All digested tissues were discharged to another tube containing 5 ml Dulbeccco's Modified Eagle Medium (DMEM; Gibco) and centrifuged at 2,000 rpm for 5 min. The liquid fat and medium at the top of the tube were removed. DMEM containing 15 % fetal bovine serum (Gibco) was added to the pellet, mixed well, and transferred to a

six-well plate. Cultures were maintained in a tissue culture incubator at 37 °C with 5 % CO_2. Mesenchymal stem cells were adhered to the surface and the red blood cells were suspended. The first medium change was performed after 2 days to remove the hematopoietic and other unattached cells, and twice a week thereafter. When the hMSCs reached 80–90 % confluence, they were trypsinized and passaged. In the third or fourth passage, hMSCs were detached with 0.05 % trypsin containing 1 mM ethylenediaminetetraacetic acid (Sigma) and counted. A density of 5×10^4 cell/specimen was seeded onto UV-sterilized electrospun scaffolds and PVA film in a 24-well plate for MTT assay and SEM observation as follows.

MTT Assay

Cell viability was indicated through the reduction of MTT (3-(4,5-dimethylthiazol-2-yl)-2,5-diphenyl tetrazolium bromide) into a formazan dye by living cells. At 3 and 7 days of cell culture on each sample, they were rinsed with PBS to remove non-adhered cells. One hundred microliters of MTT solution (0.5 mg/ml) was added to each well and incubated for 4 h under the same conditions described. Thereafter, MTT was carefully removed and 100 μl of isopropanol was added under shaking to solubilize the formazan crystals formed. The absorbance of the converted dye was recorded at 570 nm using a multiwell microplate reader (Stat Fax 2100) and normalized to the control (tissue culture polystyrene plate, Nunc Denmark) absorbance.

SEM Observations

A number of cells (5×10^4) were cultured on each sample. After 3 days of culture, cellular constructs were rinsed with PBS to remove non-adhered cells and subsequently fixed with 2.5 % GTA at 4 °C for 24 h. The samples were then dehydrated through a series of graded ethanol solutions and air-dried overnight. Dry cellular constructs were sputter coated with gold and observed with SEM.

Statistical Analysis

One-way analysis of variance, including a post hoc test for multiple comparisons, was used to statistically evaluate the PBS absorption and cell viability values. All statistical analysis were performed using IBM SPSS 16.0 software with the level of statistical significance set at $P<0.05$. Each parameter was investigated on three samples ($n=3$).

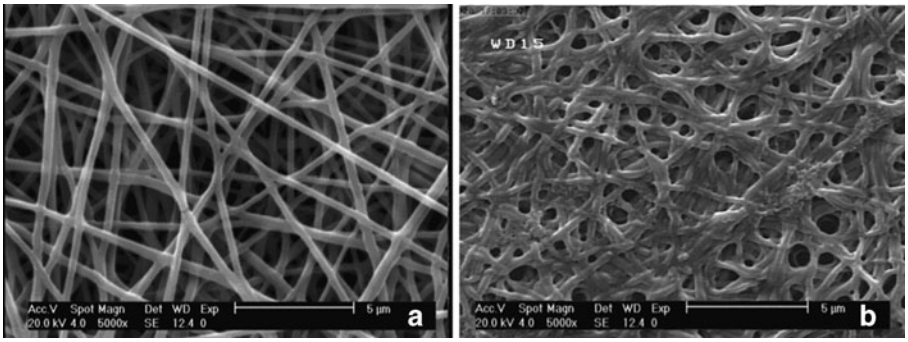

Fig. 2 Morphology of randomly oriented PVA nano-fibers **a** before and **b** after cross-linking with GTA

Results and Discussion

Morphology of Electrospun Nano-fibers

SEM micrographs revealed that highly uniform and smooth nano-fibers were formed without the occurrence of bead defects with diameter of 180±93 nm. SEM analysis showed a randomly oriented distribution of nano-fibers, when a flat collector plate was used. This is expected owing to the chaotic motion of polymeric jets of solution during the electrospinning process (Fig. 1a–b). However, when a stainless steel mesh was used as collector, it was observed that the nano-fibers have gained the same structure of the stainless steel mesh and have created a checkered pattern (Fig. 1e). The fibers appeared parallely aligned and collapsed at the wire location (Fig. 1c). Also in the space between the wires, they were almost aligned with a few fibers perpendicular to the alignment direction (Fig. 1d).

Figure 2 shows the SEM morphology of electrospun PVA nano-fibers before and after cross-linking with GTA vapor. It demonstrates that the diameter of the fibers increased after cross-linking, indicating that the fibers were swollen with water vapor present in the cross-linking solution. Evidently, exposing the fibrous matrices in the chamber caused some fibers to fuse to one another at touching points, a result of the partial dissolution of the fiber segments when they came into contact with the moisture-rich GTA vapor. A similar observation was reported for the cross-linking of the electrospun PVA fibers containing sodium salicylate as the model drug with moist GTA vapor [32].

PBS Absorption

The water absorption property of a scaffold influences not only the maintenance of the scaffold shape and form, but also affects the cells' growth. Figure 3 shows the diagram of PBS absorption of cross-linked PVA scaffolds with different surface topographies. The patterned structure had the most value with PBS absorption of 321 % and the flat film specimen had the least value with PBS absorption of 67 %. Due to the unique nano-fiber morphology with high specific surface area, the electrospun PVA substrates could absorb higher amounts of PBS compared to film structure ($p<0.05$) which is in accordance with the literature [33]. On the other hand, when the nano-fibers are collected randomly, they have a more compact structure compared to patterned nano-fibers and are intertwined irregularly; therefore, they have less free space, resulting in a less PBS absorption ($p<0.05$).

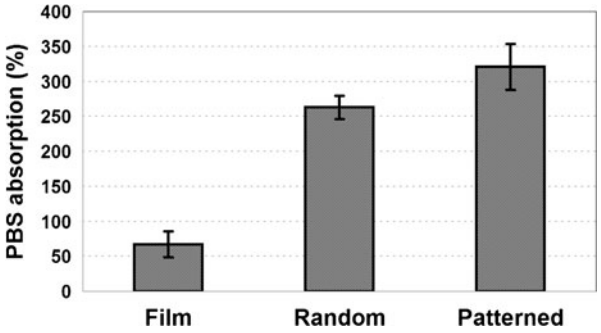

Fig. 3 PBS absorption of cross-linked scaffolds with different surface structures after 24 h

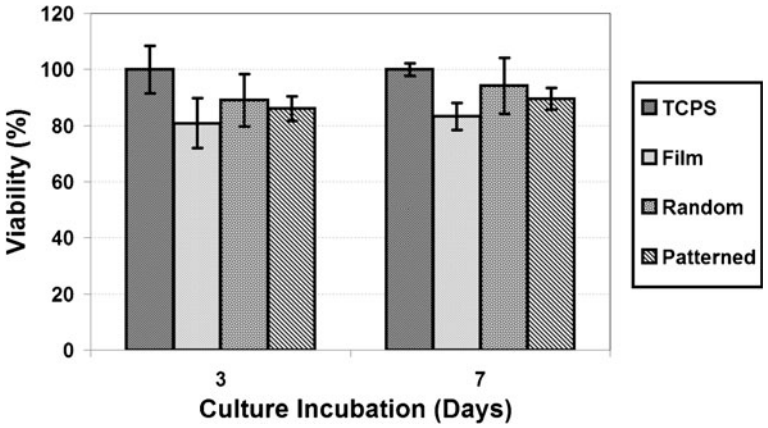

Fig. 4 Viability of hMSCs on patterned and randomly oriented PVA nano-fibers and PVA film

Cell Viability

To investigate the effect of surface nano-fibrous topography on cell viability, hMSCs were seeded onto each specimen. The MTT assay, a reliable standard test measuring cell metabolic activity as an indirect evaluation of viable cell number, was carried out after 3 and 7 days of culture on the substrates.

Figure 4 shows the viability of hMSCs when seeded on different PVA surfaces. It can be observed from the diagram that cell viability was slightly increased when seeded on PVA nano-fibrous structures (randomly oriented and patterned) compared to PVA flat film ($p>0.05$). This might be due to the large surface area of the nano-fibers available for cell attachment. Bhattarai et al. [16] also reported a similar result when they seeded chondrocytes on chitosan-PEO nano-fibrous and film substrates and observed that live cells on the nano-fibrous scaffolds appeared to be substantially more than those on the cast film. A minor increase in cell viability can also be seen on randomly oriented nano-fibers compared to patterned structure, which is not significant ($p>0.05$). Despite small differences in cell viability ($p>0.05$), the results showed that hMSCs are metabolically active in all the engineered and non-engineered surfaces.

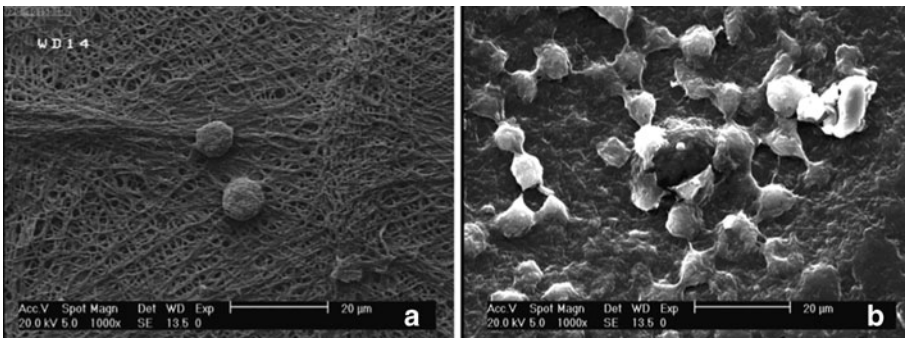

Fig. 5 SEM micrographs of hMSCs seeded on PVA nano-fibers **a** before and **b** after RGD immobilization

Cell Adhesion on RGD-Modified Nano-fibers

Various cell recognizable ligands, such as RGD peptide, galactose, and hyaluronic acid, have been grafted on the surface of porous scaffolds for tissue engineering [34, 35]. It has been reported [31, 36–39] that the RGD sequence can promote attachment of cells because it can be recognized by the adhesion receptors on the cell membrane. Thus, the affinity between cells and materials should be improved with the immobilization of RGD, which can mimic the natural ECM [40].

Figure 5 provides visual comparison of cell adhesion and density for PVA nano-fibers before and after RGD immobilization. The number of cells attached to the surface was significantly increased after RGD immobilization. After 3 days of incubation, cell morphology on unmodified PVA nano-fibers was still round-shaped while cells on RGD-modified

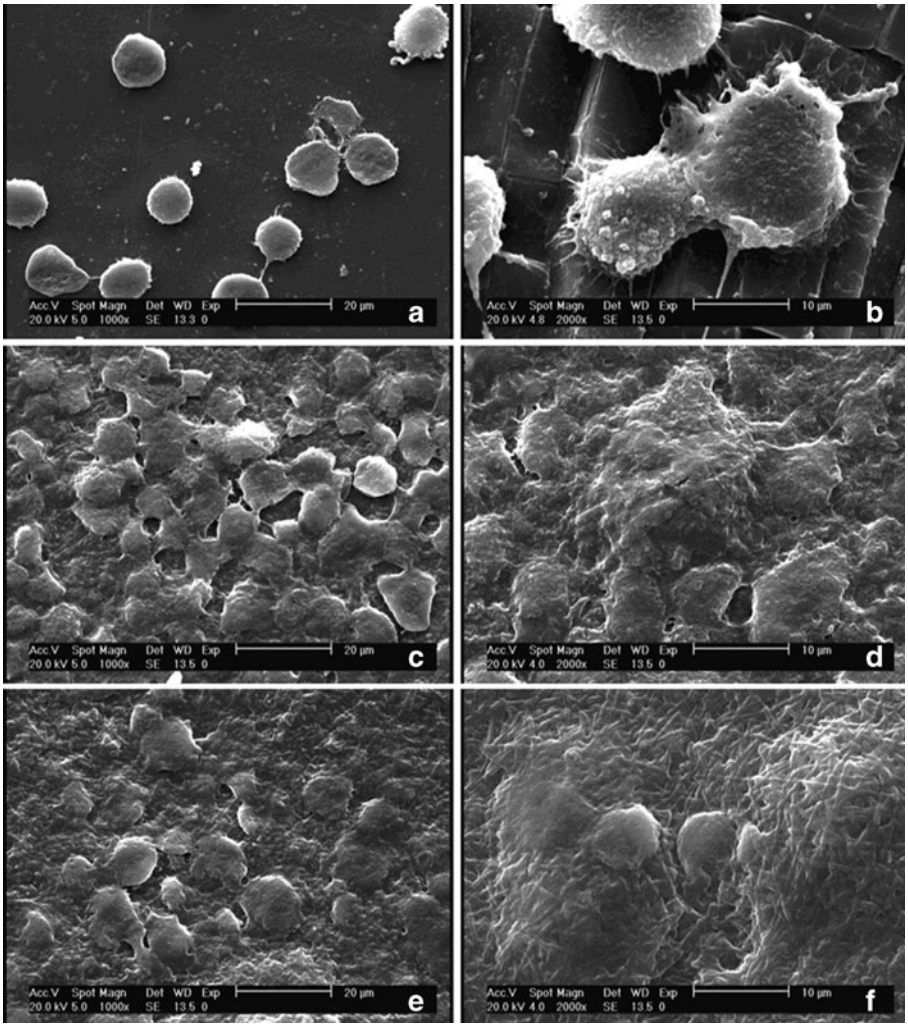

Fig. 6 SEM micrographs of hMSCs seeded on the surface of PVA film (**a** and **b**), randomly oriented nano-fibers (**c** and **d**) and patterned nano-fibers (**e** and **f**) after 3 days

matrices started to show spreading behaviors. Initial cellular adhesion and spreading events, which were initiated by the specific interaction between the immobilized ligands and cell receptors, enable the seeded cells to better adhere and communicate.

Cell Morphology

Figure 6 represents the SEM micrographs of hMSCs cultured for 3 days on different PVA scaffolds. As shown, the cell adhesion characteristics of nano-fibrous scaffolds were clearly superior to that of PVA film after culturing for 3 days. For PVA thin film materials, the cells had not adhered well or stretched, and were still considered as a ball-shaped cell (Fig. 6a); while they had spread and adhered to the surface of electrospun PVA nano-fibers (Fig. 6c and e) and the number of cells attached to the surface of nano-fibrous structures (especially randomly oriented nano-fibers) are significantly higher compared to PVA film. On the nano-fibrous scaffolds, cells were integrated with the surrounding fibers and tended to join together and form aggregates, indicating that nano-fibrous structures have a high biocompatibility. Guarino et al. [6] also performed a comparative study between PCL/gelatin films and electrospun nano-fibers and obtained a similar trend. The results showed that on nano-fibrous scaffolds, hMSCs were significantly flattened, and typically spread with a spindle or star-like shape morphology; whereas, they had a more globular shape and less cell spreading on PCL/gelatin films.

Figure 6b shows the anchoring of single cells to the hills and valleys of the PVA film surface resulting from RGD immobilization. Compared to Fig. 6d, which is in the same magnification, it can be observed that cells remained in a rounded and spherical shape on PVA film while they were more spread and flattened on the surface of randomly oriented nano-fibers. In case of patterned nano-fibrous scaffolds, it seems that after undergoing RGD immobilization steps, the nano-fibers have lost their ordered pattern. The checkered structure and the regular pattern that the nano-fibers had before placing them in aqueous solutions are not observable in these figures (Fig. 6e and f). Therefore, no significant difference in cell morphology was recognized between randomly oriented and patterned nano-fibrous scaffolds; although it appears that cells prefer to adhere to randomly oriented nano-fibers which are in accordance with the results of cell viability by MTT assay.

Conclusions

In the present study, randomly oriented and patterned PVA nano-fibrous scaffolds with mean fiber diameter of 180±93 nm were successfully electrospun and their characteristics were compared with flat PVA film. SEM micrographs showed that highly uniform and smooth nano-fibers were formed without the occurrence of bead defects. After cross-linking with GTA vapor for 120 h, the scaffolds could maintain mechanical properties when incubated in PBS for 24 h. PBS absorption of nano-fibrous structures, no matter randomly oriented or patterned, were significantly higher than PVA film due to highly porous architecture and high surface area-to-volume ratio. Furthermore, patterned nano-fibers could absorb more amounts of PBS compared to randomly oriented nano-fibers which can be attributed to the more compact and intertwined structure of the latter. To improve the cell adhesion characteristics, RGD cell adhesion ligand was immobilized onto the surface of the scaffolds prior to cellular studies. SEM images revealed that cell adhesion was effectively enhanced after RGD immobilization and higher cell densities were observed on RGD-modified scaffolds compared to non-modified ones. Cells maintained a spherical morphology on the surface of

PVA film but were induced to spread and flatten on the nano-fibrous scaffolds. No significant difference in cell morphology was observed between patterned and randomly oriented nano-fibers. However, the number of cells attached to the randomly oriented nano-fibers seemed to be higher than patterned nano-fibers. Patterned structure also revealed slightly lower cell viability compared to random nano-fibers.

Eventually, to confirm that the function of cells are generally improved on electrospun nano-fibrous scaffolds compared to film structures, which has been frequently reported [16, 41, 42], it was assumed that randomly oriented nano-fibers provide a more favorable surface for cells to attach and proliferate, while the potential applications of patterned nano-fibers need more specialized studies and experiments.

Acknowledgments The authors would like to acknowledge Dr. Hajir Bahrami and Dr. Adele Gholipour Kanaani from Department of Textile Chemistry and Fibers Science, Faculty of Textile Engineering, Amirkabir University of Technology for electrospinning facility and technical assistance. The valuable comments by Mr. Morteza Mehrjou at National Cell Bank, Pasteur Institute of Iran are also appreciated.

References

1. He, L., Liao, S., Quan, D., Ma, K., Chan, C., Ramakrishna, S., et al. (2010). *Acta Biomaterialia, 6*, 2960–2969.
2. Yim, E. K., Pang, S. W., & Leong, K. W. (2007). *Experimental Cell Research, 313*, 1820–1829.
3. Martinez, E., Engel, E., Planell, J. A., & Samitier, J. (2009). *Annals of Anatomy, 191*, 126–135.
4. Ranucci, C. S., & Moghe, P. V. (2001). *Journal of Biomedical Materials Research, 54*, 149–161.
5. Teixeira, A. I., Nealey, P. F., & Murphy, C. J. (2004). *Journal of Biomedical Materials Research, 71A*, 369–376.
6. Guarino, V., Alvarez-Perez, M., Cirillo, V., & Ambrosio, L. (2011). *Journal of Bioactive and Compatible Polymers, 26*, 144–160.
7. Dalby, M. J., Gadegaard, N., Tare, R., Andar, A., Riehle, M. O., Herzyk, P., et al. (2007). *Nature Materials, 6*, 997–1003.
8. Curtis, A. S., Gadegaard, N., Dalby, M. J., Riehle, M. O., Wilkinson, C. D., & Aitchison, G. (2004). *IEEE Transactions on NanoBioscience, 3*, 61–65.
9. Kim, T. G., & Park, T. G. (2006). *Tissue Engineering, 12*, 221–233.
10. Lee, S. Y., Jang, D. H., Kang, Y. O., Kim, O. B., Jeong, L., Kang, H. K., et al. (2012). *Applied Surface Science, 258*, 6914–6922.
11. Hersel, U., Dahmen, C., & Kessler, H. (2003). *Biomaterials, 24*, 4385–4415.
12. Barnes, C. P., Sell, S. A., Boland, E. D., Simpson, D. G., & Bowlin, G. L. (2007). *Advanced Drug Delivery Reviews, 59*, 1413–1433.
13. Lee, K. Y., Jeong, L., Kang, Y. O., Lee, S. J., & Park, W. H. (2009). *Advanced Drug Delivery Reviews, 61*, 1020–1032.
14. Smith, L. A., & Ma, P. X. (2004). *Colloids and Surfaces, B: Biointerfaces, 39*, 125–131.
15. Giannoni, P., & Narcisi, R. (2009). *Journal of Applied Biomaterials & Biomechanics, 1*, 1–12.
16. Bhattarai, N., Edmondson, D., Veiseh, O., Matsen, F. A., & Zhang, M. (2005). *Biomaterials, 26*, 6176–6184.
17. Zhang, X., Reagan, M. R., & Kaplan, D. L. (2009). *Advanced Drug Delivery Reviews, 61*, 988–1006.
18. Asran, A. S., Henning, S., & Michler, G. H. (2010). *Polymer, 51*, 868–876.
19. Sequeira, S. J., Soscia, D. A., Oztan, B., Mosier, A. P., Jean-Gilles, R., Gadre, A., et al. (2012). *Biomaterials, 33*, 3175–3186.
20. Yoshimoto, H., Shin, Y. M., Terai, H., & Vacanti, J. P. (2003). *Biomaterials, 24*, 2077–2082.
21. Peng, F., Yu, X., & Wei, M. (2011). *Acta Biomaterialia, 7*, 2585–2592.
22. Chun, J. Y., Kang, H. K., Jeong, L., Kang, Y. O., Oh, J. E., Yeo, I. S., et al. (2010). *Colloids and Surfaces, B: Biointerfaces, 78*, 334–342.
23. Wilkinson, C. D., Riehle, M. O., Wood, M., Gallagher, J., & Curtis, A. S. (2002). *Materials Science and Engineering: C, 19*, 263–269.
24. Andersson, A. S., Bäckhed, F., von Euler, A., Richter-Dahlfors, A., Sutherland, D., & Kasemo, B. (2003). *Biomaterials, 24*, 3427–3436.

25. Dalby, M. J., McCloy, D., Robertson, M., Agheli, H., Sutherland, D., Affrossman, S., et al. (2006). *Biomaterials, 27*, 2980–2987.
26. Pham, Q. P., Sharma, U., & Mikos, A. G. (2006). *Biomacromolecules, 7*, 2796–2805.
27. Coutinho, D. F., Gomes, M. E., Neves, N. M., & Reis, R. L. (2012). *Acta Biomaterialia, 8*, 1490–1497.
28. Gil, E. S., Park, S. H., Marchant, J., Omenetto, F., & Kaplan, D. L. (2010). *Macromolecular Bioscience, 10*, 664–673.
29. Koski, A., Yim, K., & Shivkumar, S. (2004). *Materials Letters, 58*, 493–497.
30. Yang, E., Qin, X., & Wang, S. (2008). *Materials Letters, 62*, 3555–3557.
31. Massia, S. P., & Hubbell, J. A. (1990). *Analytical Biochemistry, 187*, 292–301.
32. Taepaiboon, P., Rungsardthong, U., Supaphol, P. (2007) Nanotechnology 18, 175102 (11pp).
33. Liang, D., Hsiao, B. S., & Chu, B. (2007). *Advanced Drug Delivery Reviews, 59*, 1392–1412.
34. Park, T. G. (2002). *Journal of Biomedical Materials Research, 59*, 127–135.
35. Yoon, J. J., Nam, Y. S., Kim, J. H., & Park, T. G. (2002). *Biotechnology and Bioengineering, 78*, 1–10.
36. Schugens, C. H., Grandfils, C. H., Jerome, R., Teyssie, P., Delree, P., Martin, D., et al. (1992). *Journal of Biomedical Materials Research, 29*, 1349–1362.
37. Albelda, S. M., & Buck, C. A. (1990). *FASEB Journal, 4*, 2868–2680.
38. Massia, S. P., & Hubbell, J. A. (1991). *Journal of Cell Biology, 114*, 1089–1100.
39. Drumheller, P. D., Elbert, D. E., & Hubbell, J. A. (1993). *Biotechnology and Bioengineering, 43*, 772–780.
40. Ho, M. H., Wang, D. M., & Hsieh, H. J. (2005). *Biomaterials, 26*, 3197–3206.
41. Chu, X. H., Shi, X. L., Feng, Z. Q., Gu, Z., & Ding, Y. T. (2009). *Biotechnology Letters, 31*, 347–352.
42. Ho, M. H., Wang, D. M., Hsieh, H. J., Liu, H. C., Hsien, T. Y., Lai, J. Y., et al. (2005). *Biomaterials, 26*, 3197–3206.